PHYSICAL REVIEW B **76**, 121101(R) (2007)

Response of a cylindrical invisibility cloak to electromagnetic waves

Baile Zhang, Hongsheng Chen,* Bae-Ian Wu, Yu Luo, Lixin Ran, and Jin Au Kong
Research Laboratory of Electronics, Massachusetts Institute of Technology, Cambridge, Massachusetts 02139, USA
and The Electromagnetics Academy at Zhejiang University, Zhejiang University, Hangzhou 310058, China
(Received 17 July 2007; revised manuscript received 13 August 2007; published 4 September 2007)

Based on electromagnetic wave scattering theory, we demonstrate that magnetic and electric surface currents are induced at the inner boundary of a cylindrical cloak by incoming waves. These surface currents have no counterparts in the coordinate transform theory. In addition, electromagnetic fields can penetrate into the concealed region under specified conditions, but carry no power. The field distribution can be unsymmetrical when a circularly polarized wave is obliquely incident onto the cloak. The far-field scattering for a nonideal cylindrical cloak is also theoretically addressed.

DOI: 10.1103/PhysRevB.76.121101 PACS number(s): 41.20.Jb, 42.25.Fx

Recently, invisibility cloaking based on coordinate transforms has been discussed, where empty space is transformed into a shell surrounding the object to be concealed.[1] Another method was reported where the two-dimensional (2D) Helmholtz equation is transformed to produce similar effects in the geometric limit.[2] Some related work on invisibility cloaking utilizing plasmonic resonance has also been published.[3,4] The effectiveness of a transformation-based cloak design was first confirmed computationally in the geometric optics limit,[1,5] and then in full-wave, finite-element simulations,[6,7] as well as in a full-wave spherical scattering model.[8] A practical 2D cylindrical cloak, which has been realized in experiment, showed that the cloak reduces both backscattering (reflection) and forward scattering (shadow).[9] An attempt to use scattering theory to demonstrate the perfect invisibility of the cylindrical cloak in a normally incident (or 2D) case was also made in Ref. 10. However, the basic physics behind the cloaking phenomenon of a cylindrical cloak, for example, the peculiar behavior of the inner boundary of the cloak in response to incoming waves, the field distribution, and the far-field scattering behavior due to an obliquely incident wave with arbitrary polarization, and the question of whether fields can penetrate into the concealed region, is still unsolved.

In this paper, a general derivation based on the full-wave scattering model for a cylindrical cloak under oblique incidence is presented. The scattering field from an ideal cylindrical cloak with parameters obtained in Refs. 1 and 6 is shown to be indeed zero, not only in the normal incidence case,[10] but also in the oblique incidence case, corroborating the effectiveness of the cloak design process specified in Ref. 1. Meanwhile, the electromagnetic fields across the inner boundary of such a cloak are discontinuous, and at the inner boundary of the cloak, electric and magnetic surface currents along the ϕ direction, which are not predicted by the coordinate transform theory, will be induced. This indicates that a full-wave analytical scattering calculation is very necessary for further investigation of the response of the cloak with a peculiar inner boundary. Extending the inner boundary inward will cause the fields, but not the power, to penetrate into the concealed region. In addition, the field distribution due to a circularly polarized incident wave can be unsymmetrical while the power is still distributed symmetrically. The sensitivity of the cloak to nonideal parameters is also discussed. All of these aspects provide us with deeper insights into the cloaking phenomenon.

Figure 1 shows the configuration of the scattering from a cylindrical cloak with outer radius R_2 and inner radius R_1 on which a time-harmonic plane wave $\bar{E}_i$ is obliquely incident. Let $\bar{E}_i=(\hat{v}_i E_{vi}+\hat{h}_i E_{hi})e^{i\bar{k}\cdot\bar{r}}$, where $\bar{k}=\hat{x}k_\rho+\hat{z}k_z$, $k^2=\omega^2\mu_0\epsilon_0$, $\hat{h}_i=\hat{z}\times\hat{k}/|\hat{z}\times\hat{k}|$, and $\hat{v}_i=\hat{h}_i\times\hat{k}$.[11] Without loss of generality, we assume that the concealed region is filled with an isotropic material with permittivity ϵ_2 and permeability μ_2. The cloak layer between R_1 and R_2 is a specific anisotropic and inhomogeneous medium with permittivity tensor $\bar{\bar{\epsilon}}=\epsilon_\rho\hat{\rho}\hat{\rho}+\epsilon_\phi\hat{\phi}\hat{\phi}+\epsilon_z\hat{z}\hat{z}$ and permeability tensor $\bar{\bar{\mu}}=\mu_\rho\hat{\rho}\hat{\rho}+\mu_\phi\hat{\phi}\hat{\phi}+\mu_z\hat{z}\hat{z}$. According to Refs. 6 and 9, we choose $\epsilon_\rho/\epsilon_1=\mu_\rho/\mu_1=(\rho-R_1)/\rho$, $\epsilon_\phi/\epsilon_1=\mu_\phi/\mu_1=\rho/(\rho-R_1)$, and $\epsilon_z/\epsilon_1=\mu_z/\mu_1=[R_2/(R_2-R_1)^2](\rho-R_1)/\rho$. When $\epsilon_1=\epsilon_0$ and $\mu_1=\mu_0$, the cloak corresponds to the ideal cloak.

In a source-free medium, the fields can be decomposed into TE^z and TM^z modes with respect to $\hat{z}$,[12] corresponding to scalar potentials ψ^z_{TM} and ψ^z_{TE}, respectively,

$$\bar{H}_{TM}=\bar{\bar{\mu}}^{-1}\cdot\nabla\times(\hat{z}\psi^z_{TM}), \tag{1a}$$

$$\bar{E}_{TE}=-\bar{\bar{\epsilon}}^{-1}\cdot\nabla\times(\hat{z}\psi^z_{TE}), \tag{1b}$$

$$\bar{E}_{TM}=\frac{1}{-i\omega}\bar{\bar{\epsilon}}^{-1}\cdot[\bar{\bar{\mu}}^{-1}\cdot\nabla\times(\hat{z}\psi^z_{TM})], \tag{1c}$$

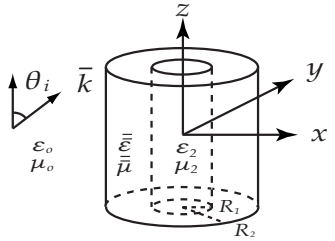

FIG. 1. Geometry of a cylindrical cloak. The incident wave propagates in the direction of $\bar{k}$.

$$\bar{H}_{TE} = \frac{1}{-i\omega}\bar{\bar{\mu}}^{-1} \cdot [\bar{\bar{\epsilon}}^{-1} \cdot \nabla \times (\hat{z}\psi_{TE}^{z})]. \tag{1d}$$

Hereafter the superscript z is suppressed. After substituting Eqs. (1) into the Maxwell equations, we can get the wave equation for the scalar potentials as follows:

$$\frac{1}{\rho - R_1}\frac{\partial}{\partial \rho}(\rho - R_1)\frac{\partial \psi}{\partial \rho} + \frac{1}{(\rho - R_1)^2}\frac{\partial^2 \psi}{\partial \phi^2} + \frac{R_2^2}{(R_2 - R_1)^2}\left(\omega^2 \mu_1 \epsilon_1 \psi + \frac{\partial^2 \psi}{\partial z^2}\right) = 0. \tag{2}$$

Using the method of separation of variables, the general expression for the two scalar potentials is obtained as

$$\psi = B_n\left(R_2 k_{\rho 1}\frac{(\rho - R_1)}{(R_2 - R_1)}\right)e^{in\phi + ik_z z}, \tag{3}$$

where B_n represents the solutions of the Bessel equation of nth order, and $k_{\rho 1} = \sqrt{\omega^2 \epsilon_1 \mu_1 - k_z^2} = \sqrt{k_1^2 - k_z^2}$. As in the spherical cloak,[8] the scalar potentials ψ^i, ψ^s, ψ^c, and ψ^{int} for the incident fields ($\rho > R_2$), the scattered fields ($\rho > R_2$), the fields inside the cloak layer ($R_1 < \rho < R_2$) and the internal fields ($\rho < R_1$), respectively, for both TE and TM waves, can be represented. By matching the boundary conditions, all the expanding coefficients of these scalar potentials can be deduced.

For convenience of demonstration, we first consider the simple TM case where a vertically polarized (E_z) plane wave is normally incident onto an ideal cylindrical cloak, i.e., $k_z = 0$ and $E_{hi} = 0$ as well as $\mu_1 = \mu_0$ and $\epsilon_1 = \epsilon_0$, which appears in Refs. 6, 9, and 10. In order to match the boundary conditions, the inner boundary of the cloak is set at $\rho = R_1 + \delta$ instead of $\rho = R_1$ and then the limit $\delta \to 0$ is taken[10] while the parameters of the cloak are still unchanged. Consequently, four boundary equations can be listed, utilizing the continuities of E_z and H_ϕ at the outer boundary [Eqs. (4) and (5)] and at the inner boundary [Eqs. (6) and (7)]:

$$-\frac{i^{n-1}}{\omega}E_{vi}J_n(kR_2) + a_n^{(M)}H_n(kR_2) = d_n^{(M)}J_n(kR_2) + f_n^{(M)}N_n(kR_2), \tag{4}$$

$$-\frac{i^{n-1}}{\omega}E_{vi}J_n'(kR_2) + a_n^{(M)}H_n'(kR_2) = d_n^{(M)}J_n'(kR_2) + f_n^{(M)}N_n'(kR_2), \tag{5}$$

$$d_n^{(M)}J_n\left(\frac{R_2}{R_2 - R_1}k\delta\right) + f_n^{(M)}N_n\left(\frac{R_2}{R_2 - R_1}k\delta\right) = g_n^{(M)}J_n(k_2 R_1), \tag{6}$$

$$\frac{R_2\delta}{(R_2 - R_1)R_1}\left[d_n^{(M)}J_n'\left(\frac{R_2}{R_2 - R_1}k\delta\right) + f_n^{(M)}N_n'\left(\frac{R_2}{R_2 - R_1}k\delta\right)\right] = \sqrt{\frac{\mu_0 \epsilon_2}{\epsilon_0 \mu_2}}g_n^{(M)}J_n'(k_2 R_1), \tag{7}$$

where J_n, N_n, and H_n represent the nth-order Bessel function, the Neumann function, and the Hankel function of the first kind, respectively; $a_n^{(M)}$, $g_n^{(M)}$, $d_n^{(M)}$, and $f_n^{(M)}$ are unknown coefficients corresponding to the scattering field, the internal field, and the field inside the cloak, respectively. After solving all the equations, it is seen that $a_n^{(M)} = f_n^{(M)} = g_n^{(M)} = 0$, indicating that both the internal field and the scattering field are zero. The most interesting thing that is not shown in Ref. 10 is that, when $n = 0$, though $f_0^{(M)} = 0$, the product $f_0^{(M)}N_0\{[R_2/(R_2 - R_1)]k\delta\}$ in the limit $\delta \to 0$ is equal to $E_{vi}/i\omega$. Obviously, the value of this product in Eq. (6) is nonzero only at the inner boundary, which can be characterized as a magnetic surface current raised by the infinite μ_ϕ at the inner boundary of the cloak. Since the tangential electric field on the cloak side of the inner boundary is E_{vi}, the magnetic surface current with an amplitude E_{vi} shields the concealed object, making the field inside exactly zero. Reference 10 mentioned the "slow convergence" of the scattering coefficients but did not note that this is actually due to the surface current at the inner boundary. It also should be pointed out that this surface current is a property of the material at the inner boundary itself, being different from the active and nonlocal surface sources added artificially for cloaking discussed in Ref. 13.

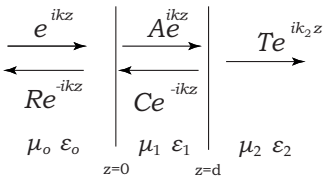

FIG. 2. Three-layer model with a normally incident wave for demonstrating the surface currents at the inner boundary of a cylindrical cloak. The slab's permeability μ_1 goes to infinity while the permittivity goes to zero, but their product is kept equal to $\mu_0\epsilon_0$.

In order to further reveal the properties of this surface current, let us first consider a simplified case as shown in Fig. 2, where a plane wave $E_i = E_0 e^{ikz}$ is normally incident onto a slab with $\epsilon_1 \to 0$ and $\mu_1 \to \infty$ but $\mu_1\epsilon_1 = \mu_0\epsilon_0$. This special material has the same properties as those at the inner boundary of a cylindrical cloak, where $\epsilon_z = 0$ and $\mu_\phi = \infty$ but $\epsilon_z\mu_\phi = [R_2/(R_2 - R_1)^2]$. It is easy to obtain that $R = 1$ and $T = 0$. The elctric field at $z = 0$ is $2E_0$ while that at $z = d$ is zero. Meanwhile, $\int_0^d i\omega B\, dz$ is exactly equal to $2E_0$. Therefore this slab acts like a perfect magnetic conductor (PMC) but it is the volume displacement current that is distributed in the slab. When the thickness of the slab becomes infinitesimal, the volume displacement current becomes a surface displacement current.

Similarly, we can introduce a third boundary at $\rho = R_0$ ($R_0 < R_1$) as shown in Fig. 3. The region between $R_0 < \rho < R_1$ is filled with the same material as the inner boundary at $\rho = R_1$, i.e., the region $R_0 < \rho < R_1$ is homogeneous, like the slab in Fig. 2. The calculated electric field and the Poynting power due to an E_z-polarized wave normally incident onto an ideal cylindrical cloak but with such an extended inner boundary are shown in Fig. 3. It is seen that there is no field in the region of $\rho < R_0$, but the E_z field in the region $R_0 < \rho < R_1$ is nonzero. The integration $\int_{R_0}^{R_1} i\omega B_\phi d\rho$ is the total magnetic current in this region, which has a value of

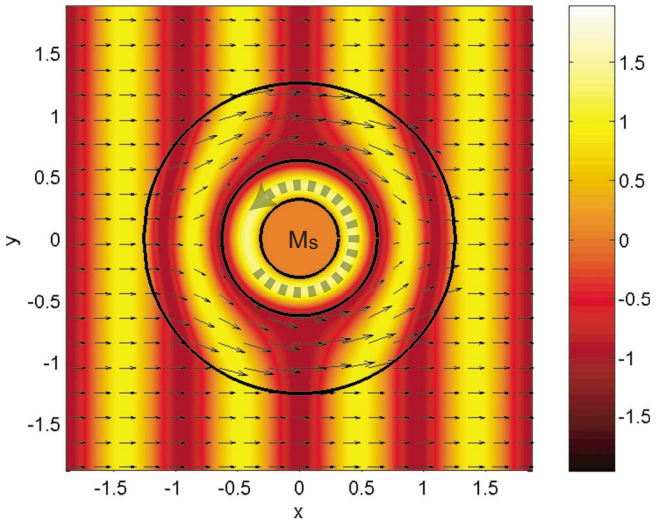

FIG. 3. (Color online) Field distribution of E_z in the xy plane due to an E_z-polarized wave normally incident onto a cylindrical cloak but with the inner boundary extended inward. The radii of the three concentric circles are $R_2=1.33\lambda_0$, $R_1=R_2/2$, and $R_0=R_2/4$, respectively. The arrows represent the Poynting vectors in the xy plane.

E_z, equal to the surface magnetic current when $\rho=R_0$ and $\rho=R_1$ overlap, as we mentioned before. In other words, the surface magnetic current M_s that was previously concentrated at the boundary of $\rho=R_1$ in the case of $R_0=R_1$ is now distributed over the region $R_0<\rho<R_1$. It should be noted that, with the inner boundary extended (i.e., $R_0<R_1$), B_ϕ at $\rho=R_1$ is finite, while in the case when $\rho=R_0$ and $\rho=R_1$ overlap (i.e., $R_0=R_1$), B_ϕ at $\rho=R_1$ becomes divergent. Therefore, the field at the inner boundary $\rho=R_1$ is dependent on the material in the region of $\rho<R_1$, which means it cannot be determined by the coordinate transform method.[1] In addition, although the field can penetrate through the boundary $\rho=R_1$ in this specific case, the Poynting power along the r direction, P_r is always zero (because H_ϕ is always zero in this region), and no power can penetrate into the concealed region. In addition, compared with the spherical cloak where the tangential Poynting power decreases to zero at the inner boundary,[8] for a cylindrical cloak not all of the tangential Poynting power P_ϕ at $\rho=R_1$ is zero.

For a general obliquely incident plane wave with arbitrary polarization, all the coefficients of TM and TE modes can be derived in the same way. Figure 4 shows the distribution of the E_x component and Poynting power in the xy and xz planes when a right-handed circularly polarized wave is incident at $\theta_i=45°$. It is seen that perfect invisibility can still be obtained for obliquely incident waves, indicating that the cylindrical cloaking is not limited to the 2D case only.[6,9,10] Oblique rays traversing a cylindrical cloak have also been shown in Ref. 5, but were in the geometric limit. We can conclude that, in order to completely shield a 3D concealed object, the cylindrical cloak must be infinitely long. In practice, we have to rely on a finite-sized cloak. Obviously, the longer the cylinder, the better the cloaking performance. It is also worth mentioning that, in the xy plane, the fields inside the cloak are no longer symmetric with respect to the x axis,

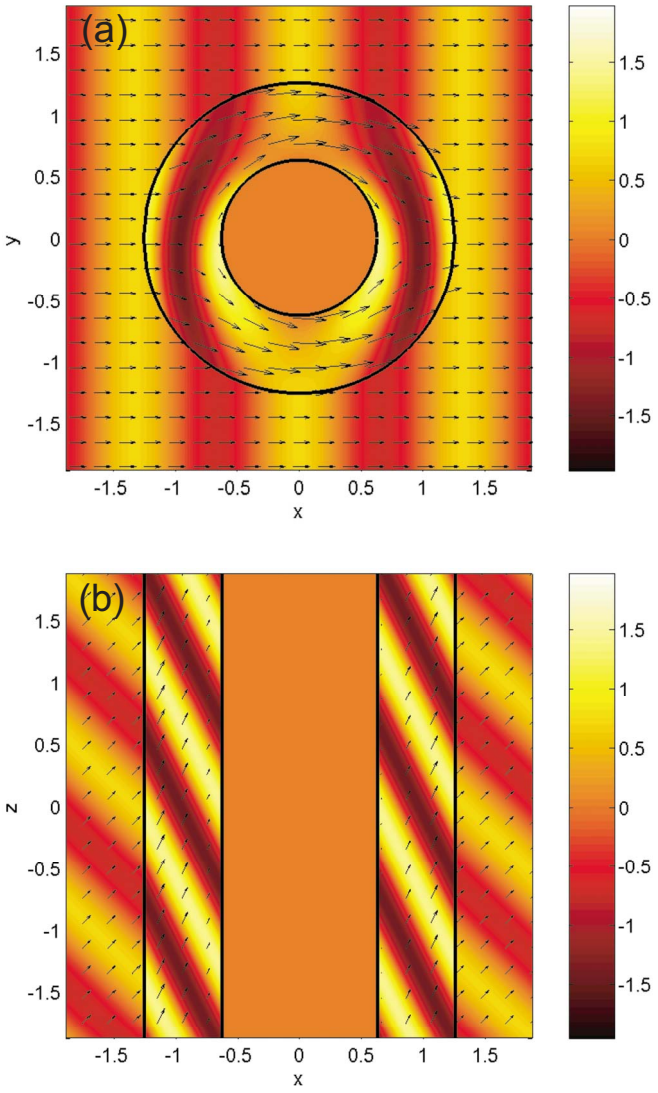

FIG. 4. (Color online) Field distribution of E_x in the (a) xy and (b) xz plane due to a right-handed circularly polarized incident wave with 45° incident angle. The cloak has the size $R_2=1.33\lambda_0$ and $R_1=R_2/2$. The arrows represent the directions of the Poynting vectors.

while the flowing power is still distributed symmetrically. This special distribution property is unique for an obliquely incident wave having both vertical and horizontal polarizations. In addition, the discontinuities of E_z and H_z across the inner boundary can be similarly attributed to the electric and magnetic surface currents at the inner boundary of the cloak. For the ideal cylindrical cloak where $\mu_1=\mu_0$ and $\epsilon_1=\epsilon_0$, the discontinuities are $(E_{hi}/\eta_0)\sin\theta_i e^{ik_z z}$ and $E_{vi}\sin\theta_t e^{ik_z z}$, which are exactly the vertical components of the incident magnetic and electrical fields, respectively.

This phenomenon arises from the coordinate transformation process. In a spherical cloak, the coordinate transformation approach transforms a field vector at the origin into radial components at the inner boundary. However, this transformation in a cylindrical cloak only applies to the transverse components in the xy plane but does not do anything to the vertical component, because the transform coef-

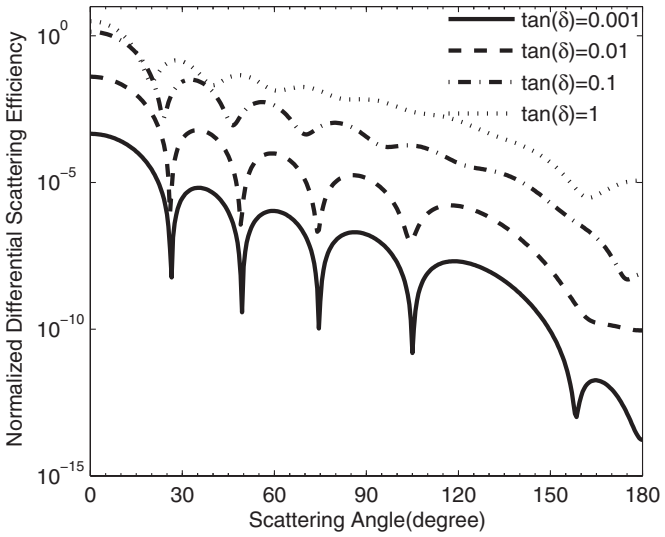

FIG. 5. Scattering pattern in the *xy* plane due to a vertically polarized and normally incident wave with different loss tangents for each component of the constitutive parameters. The configuration of the cloak is the same as that shown in the caption of Fig. 4.

ficient for the z component, Q_z,[1,14] is equal to 1. Therefore, there must be a discontinuity across the inner boundary which induces a surface current if we assume no field exists inside the core. These surface currents do not exist before the transformation and have no counterpoints in the original Cartesian coordinate system.

Based on the cylindrical scattering model, the far-field scattering efficiency Q_{sca},[15] or the scattering cross section normalized by the geometrical cross section, for a cylindrical cloak with nonideal parameters can be calculated correspondingly. When a loss tangent is included in each component of the cloak's constitutive parameters, the scattering fields become nonzero. Figure 5 plots the differential scattering efficiency of an E_z-polarized and normally incident wave as a function of the scattering angle in the xy plane for loss tangents of 0.001, 0.01, 0.1, and 1, respectively. Generally, with increasing loss, the scattering increases. However, the backward scattering ($\phi=180°$) is not absolutely zero, which is different from the spherical cloak with the same specific kind of loss.[8] Second, the scattering angle where the minimum scattering occurs is no longer located at 180° as the loss tangent increases. The sensitivity of the performance of the cylindrical cloak to the mismatches ($\mu_1/\epsilon_1 \neq \eta_0$) of the constitutive parameters can also be quantitatively calculated by the presented full-wave cylindrical scattering model. Since the property is very similar to that of the spherical cloak,[8] we will not elaborate this case here.

In conclusion, we showed that electric and magnetic surface currents will be induced at the inner boundary of a cylindrical cloak by incoming electromagnetic waves, and these surface currents have no counterparts in the coordinate transformation. In a special configuration where the inner boundary is extended inward, the fields but not the power can penetrate into the concealed region. Invisibility under obliquely incident waves with arbitrary polarization is also demonstrated. The effect of nonideal parameters on the cloaking performance is theoretically analyzed. These aspects of the cylindrical cloak are important for developing further physical insights into the cloaking phenomenon.

This work is sponsored by the ONR under Contract No. N00014-01-1-0713, the Department of the Air Force under Air Force Contract No. F19628-00-C-0002, the Chinese NSF under Grant No. 60531020, and China PSF under Grant No. 20060390331.

*Corresponding author; chenhs@ewt.mit.edu

[1] J. B. Pendry, D. Schurig, and D. R. Smith, Science **312**, 1780 (2006).
[2] U. Leonhardt, Science **312**, 1777 (2006).
[3] A. Alu and N. Engheta, Phys. Rev. E **72**, 016623 (2005).
[4] G. W. Milton and N.-A. P. Nicorovici, Proc. R. Soc. London, Ser. A **462**, 3027 (2006).
[5] D. Schurig, J. B. Pendry, and D. R. Smith, Opt. Express **14**, 9794 (2006).
[6] S. A. Cummer, B.-I. Popa, D. Schurig, D. R. Smith, and J. B. Pendry, Phys. Rev. E **74**, 036621 (2006).
[7] F. Zolla, S. Guenneau, A. Nicolet, and J. B. Pendry, Opt. Lett. **32**, 1069 (2007).
[8] H. Chen, B. I. Wu, B. Zhang, and J. A. Kong, Phys. Rev. Lett. **99**, 063903 (2007).
[9] D. Schurig, J. J. Mock, B. J. Justice, S. A. Cummer, J. B. Pendry, A. F. Starr, and D. R. Smith, Science **314**, 977 (2006).
[10] Z. Ruan, M. Yan, C. W. Neff, and M. Qiu, arXiv:0704.1183v2 Phys. Rev. Lett. (to be published).
[11] L. Tsang, J. A. Kong, and K. H. Ding, *Scattering of Electromagnetic Waves* (Wiley, New York, 2000), Vol. 1.
[12] W. Chew, *Waves and Fields in Inhomogeneous Media*, 2nd ed. (IEEE Press, New York, 1995).
[13] D. A. B. Miller, Opt. Express **14**, 12457 (2006).
[14] A. J. Ward and J. B. Pendry, J. Mod. Opt. **43**, 773 (1996).
[15]
$$Q_{sca} = \frac{2\omega\eta_0 \sin\theta_i}{(E_{vi}^2 + E_{hi}^2)R_2} \times \left(\frac{1}{\epsilon_1} \sum_{n=-\infty}^{\infty} |a_n^{(N)}|^2 + \frac{1}{\mu_1} \sum_{n=-\infty}^{\infty} |a_n^{(M)}|^2 \right).$$